Published in final edited form as:
Heart Rhythm. 2014 January ; 11(1): 85–92. doi:10.1016/j.hrthm.2013.10.007.

Magnetic Resonance Image Intensity Ratio, A Normalized Measure to Enable Inter-Patient Comparability of Left Atrial Fibrosis

Irfan M. Khurram, MD[1], **Roy Beinart, MD**[1], **Vadim Zipunnikov, PhD**[2], **Jane Dewire, BA**[1], **Hirad Yarmohammadi, MD, MPH**[1], **Takeshi Sasaki, MD**[1], **David D. Spragg, MD**[1], **Joseph E. Marine, MD**[1], **Ronald D. Berger, MD, PhD, FHRS**[1], **Henry R. Halperin, MD, MA, FHRS**[1,3], **Hugh Calkins, MD, FHRS**[1], **Stefan L. Zimmerman, MD**[3], and **Saman Nazarian, MD, PhD, FHRS**[1]

[1] Department of Medicine/Cardiology, Johns Hopkins University, Baltimore, MD

[2] Department of Biostatistics, Johns Hopkins University, Baltimore, MD

[3] Department of Radiology, Johns Hopkins University, Baltimore, MD

Abstract

Background—The measurement of late gadolinium enhanced MRI (LGE-MRI) intensity in arbitrary units (au), limits the objectivity of thresholds for focal scar detection and inter-patient comparisons of scar burden.

Objective—We sought to develop and validate a normalized measure, the image intensity ratio (IIR), for assessment of left atrial (LA) scar on LGE-MRI.

Methods—ECG- and respiratory-gated 1.5 Tesla LGE-MRI was performed in 75 patients (75% male, 62±8 years) prior to atrial fibrillation (AF) ablation. The local IIR was defined as LA myocardial signal intensity for each of 20 sectors on contiguous axial image planes divided by the mean LA blood pool image intensity. Intra-cardiac point-by-point sampled electro-anatomical map (EAM) points were co-registered with corresponding image sectors.

Results—The average bipolar voltage for all 8,153 EAM points was 0.9±1.1 mV. In a mixed effects model accounting for within patient clustering, and adjusting for age, LA volume and mass, body mass index, gender, CHA_2DS_2-VASc score, AF type, history of previous ablations, and contrast delay time, each unit increase in local IIR was associated with 91.3% decrease in bipolar LA voltage (P<0.001). Local IIR thresholds of >0.97 and >1.61 corresponded to bipolar voltage <0.5 mV and <0.1 mV, respectively.

Conclusion—Normalization of LGE-MRI intensity by the mean blood pool intensity results in a metric that is closely associated with intra-cardiac voltage as a surrogate of atrial fibrosis.

Address for Correspondence: Saman Nazarian, MD, PhD Johns Hopkins University Carnegie 592A, 600 N. Wolfe Street, Baltimore, MD 21287 Phone: 410-614-2751; Fax: 410-502-4854 snazarian@jhmi.edu.

Disclosures: Dr. Nazarian is on the MRI advisory panel for Medtronic, and is a scientific advisor to and principal investigator for research funding to Johns Hopkins University from Biosense-Webster Inc.

Keywords

atrial fibrillation; scar; late-gadolinium enhanced magnetic resonance imaging; electroanatomic mapping

Introduction

Catheter ablation is frequently performed for treatment of atrial fibrillation (AF).[1] Prior studies have revealed that late gadolinium enhancement (LGE) on magnetic resonance imaging (MRI) can noninvasively estimate the extent of LA scar before and after ablation,[2, 3] and that AF recurrence following ablation is associated with the extent of pre-ablation LGE as a surrogate of left atrial (LA) scar.[4] In a recent issue of the Journal we provided evidence to support the utility of T1 mapping for quantification of *diffuse* atrial scar.[5] Nonetheless, LGE-MRI remains necessary for identification of *focal* scar. An intrinsic limitation of LGE, however, is that MRI signal intensity is measured in "arbitrary units" (au) with variable magnitude and scale across examinations. Although LA wall image intensity on LGE-MRI primarily varies as a function of gadolinium retention in fibrotic regions, it is also affected by parameters such as surface coil proximity, contrast dose, delay time of image acquisition after contrast injection, patient hematocrit, glomerular filtration rate, and body mass index (BMI).[6, 7] Normalization of the image intensity may decrease the variability of measurement with regard to the latter covariates. The aims of this study were a) to develop the image intensity ratio (IIR) as a quantitative and normalized measure of LA fibrosis, b) to validate the IIR against invasive bipolar electrogram voltage amplitude measures, and c) to establish IIR thresholds for identification of abnormal LA myocardium and dense scar corresponding to bipolar voltage amplitudes <0.5 mV[8] and <0.1 mV,[9] respectively.

Methods

The protocol was reviewed and approved by our Institutional Review Board and all participants provided written informed consent. Seventy-five consecutive patients referred for AF ablation underwent pre-procedural MRI between November 2011 and December 2012.

Magnetic Resonance Imaging

Images were obtained using a 1.5 Tesla MRI scanner (Avanto, Siemens, Erlangen, Germany) and a 6-channel phased array body coil in combination with 6-channel spine matrix coil. Contrast-enhanced 3D MR angiography images were used to define LA and PV anatomy (echo time 0.8 ms, repetition time 2.2 ms, in-plane resolution 1.4 × 1.4 mm, slice thickness 1.4 mm). To optimize ablation success,[10] patients with persistent or long-standing persistent AF were started on anti-arrhythmic medications and referred for cardioversion 3-4 weeks prior to MRI and AF ablation. Of all patients, 9 (12%) were in AF at the time of scan. The MRI examination was performed using the same methodology regardless of the presenting rhythm. LGE-MRI scans were acquired within a range of 15-25 (mean 18.8±2.4) minutes following 0.2 mmol/kg gadolinium injection (gadopentetate dimeglumine; Bayer Healthcare Pharmaceuticals, Montville, NJ) using a fat-saturated 3D IR-prepared fast spoiled gradient recalled echo sequence with respiratory navigation and ECG-gating, echo time of 1.52 ms, repetition time of 3.8 ms, in-plane resolution of 1.3 × 1.3, slice thickness of 2.0 mm, and flip angle of 10 degrees. Trigger time for 3D LGE-MRI images was optimized to acquire imaging data during diastole of LA as dictated by inspection of the cine images. The optimal inversion time (TI) was identified with a TI scout scan (median 270 ms, range

240-290 ms) to maximize nulling of LA myocardium. A parallel imaging technique, Generalized Auto-calibrating Partially Parallel Acquisition (GRAPPA, reduction factor 2), was used.

Image Analysis

Images were processed off-line using QMass MR software (Version 7.2, Leiden University Medical Center, Leiden, The Netherlands) by an observer that was masked to electroanatomic map (EAM) results. Multiplanar reformatted (MPR) axial images with 3.5mm slice thickness were reconstructed from 3D axial image data. Epicardial and endocardial contours were manually drawn around LA myocardium. The reference point was placed at the posterior base of the LA septum and the LA myocardium in each axial plane was divided into 20 sectors (Figure 1a) with clockwise numbering from the reference point. The IIR for each sector, defined as the mean pixel intensity of each sector divided by the mean pixel intensity of the entire LA blood pool, was calculated. To measure inter- and intra-observer variability, the epicardial and endocardial contouring of the entire LA was repeated for a random sample of 10 patients by a second independent observer and by the primary observer, respectively.

Electroanatomic Mapping and Ablation

Patients that presented in AF were cardioverted to aid in identification of pulmonary vein potentials. Cardioversion was performed prior to image registration and EAM to minimize patient movement and registration errors. Detailed endocardial voltage mapping of the LA was performed prior to ablation and in sinus rhythm in all cases (Figure 1b). EAM was performed using the 3.5 mm tip with 2 mm inter-electrode spacing irrigated Thermocool ablation catheter and the CARTO-3 mapping system (Biosense Webster, Inc., Diamond Bar, CA). The LA angiography image was registered to the EAM using standard landmark image registration techniques (Figure 1c). Abnormal myocardium was defined as bipolar voltage amplitude <0.5 mV[8] and dense scar was defined as bipolar voltage amplitude <0.1 mV.[9] Acute pulmonary vein isolation (PVI) was achieved in all subjects. In persistent AF cases, the ablation also included linear rooflines, posterior wall debulking, cavotricuspid isthmus ablation, and superior vena cava isolation. Patients were observed for 24 hours following the procedure. No immediate postoperative complications were noted.

Image and Electrogram registration

Using previously validated custom software (Volley, Johns Hopkins University),[11, 12] intra-cardiac sampled points were registered to the LGE image based on the procedural registration coordinates of EAM merge with the LA angiogram. Figure 1 illustrates an example of EAM point registration to LGE MPR planes.

Statistical analyses

Continuous variables are expressed as mean ± standard deviation (SD) and categorical data as numbers or percentages. The unadjusted relationship between IIR and bipolar voltage was initially explored with scatterplots. Due to the skewed nature of bipolar voltage measures, log-transformation was utilized to accommodate modeling within a linear normal framework. A Generalized Estimating Equations (GEE) marginal model with exchangeable working correlation structure was utilized to examine the association between bipolar voltage and IIR. The model was clustered by patient, and adjusted for age, LA mass, LA volume, gender, CHA_2DS_2-VASc score, AF type, history of previous ablation, and the delay time between contrast injection and LGE image acquisition. The intra-class correlation coefficients for inter- and intra-observer variability in measuring the IIR were calculated using two-way random effects models. Statistical analyses were performed using STATA

(version 12, StataCorp, College Station, Texas) and lme4 and geepack packages in R statistical software (http://www.r-project.org).

Results

Patient Characteristics

We enrolled 75 patients with a mean age of 62.4±8.3 years (range: 44-73 years). Table 1 summarizes the baseline characteristics of patients. Forty-two patients (56%) had paroxysmal AF; and 43 (57.3%) were undergoing their first ablation procedure. Fifty-six patients (74.7%) were men. Eleven (14.7%) had congestive heart failure, 36 (48%) had hypertension, 5 (6.7%) had diabetes mellitus, and 4 (5.3%) had a history of transient ischemic attack or stroke. The median CHA_2DS_2-VASc score was 1 (interquartile range 1–2). Aside from shorter AF duration in patients without prior ablation (4.9±6.3 versus 8.9±6.8 years, P=0.11), there were no differences in baseline characteristics among patients with different AF types, and among patients with versus without prior ablation.

Table 2 illustrates structural LA differences among patients with different AF types and those with versus without prior ablation. Patients with paroxysmal AF had smaller LA volume index (78.3±18.9 versus 89.5±21.5 ml/m^2, P=0.019), and lower mean IIR (0.82±0.10 versus 0.89±0.11, P=0.002) than those with persistent AF. Patients without prior ablation had lower mean IIR (0.83±0.12 versus 0.88±0.08, P=0.039) than those with prior ablation.

Analyzed sectors on MRI and EAM

A total of 37,580 sectors from 1,879 LGE axial image planes from 75 patients were quantitatively analyzed. A total of 8,544 EAM points were registered to the 3D LGE images. Of these, 391 points were excluded from the study due to suboptimal catheter contact evidenced by instability in the beat-to-beat electrogram signal or poor registration (>1.5mm distance between EAM and corresponding myocardial sector). Consequently, 8,153 EAM points obtained from LA endocardium were evaluated and registered to the corresponding LGE-MRI sectors. The image intensity in arbitrary units (au) and the IIR were measured for each sector. The relationship of image intensity versus IIR and the distribution of each measure are plotted in Figure 2. In contrast to the right skewed image intensity distribution, the IIR histogram displayed a normal distribution. While image intensity and IIR measures have a linear relationship within each patient, the slope of this association varies across patients with a range of 0.01-0.16 au^{-1}. Figure 3 compares EAM voltage (Panel A), IIR (Panel B), and intensity maps with thresholds at 2 (Panel C), and 3 (Panel D) SD above the mean intensity of normal myocardium in a patient with extensive scar (top row) and another patient with minimal scar (bottom row). The distribution and proportion of scar represented by the IIR maps closely resemble results obtained from EAM. Using the dynamic intensity threshold technique (Panels C and D), the extent of scar estimation is significantly altered depending upon the choice of threshold at 2 versus 3 SD above the mean intensity of normal myocardium.

Association of IIR with Local Electrograms

The average bipolar voltage was 0.9±1.1 mV and the average IIR was 0.99±0.27. The local IIR was strongly associated with bipolar voltage (P<0.001); however, the relationship was more linear with log transformation of bipolar voltage measures (Figure 4, P<0.001). Individual linear and non-parametrically smoothed IIR versus log bipolar voltage relationships for each patient are demonstrated in Figure 5. Individual panels in this figure show the important finding that a linear association between log-bipolar voltage and the IIR exists in individual patients. Using a GEE model clustered by patient and adjusting for age,

LA volume, gender, CHA_2DS_2-VASc score, and the type of AF, the presence or absence of previous ablations, and the delay time, each unit increase in local IIR was associated with 91.3% decrease in local bipolar LA voltage (P<0.0001). Based upon unadjusted analyses, local IIR thresholds of >0.97 and >1.61 corresponded to bipolar voltage <0.5 mV and <0.1 mV, respectively. The uncertainty associated with each IIR threshold based upon the final sample size of 75 patients is graphically displayed in Supplemental Figure 1.

Inter- and intra-observer variability

A total of 4420 sectors from 221 LGE-MRI axial planes from 10 patients underwent repeat review for assessment of inter- and intra-observer variability (Supplemental Figure 2). The intra-class correlations for inter-reader variability of the IIR measures were 0.969 for reliability of observations (95% CI: 0.967-0.971). The intra-class correlations for intra-reader variability of the IIR measures were 0.977 for reliability of observations (95% CI: 0.975-0.978).

Discussion

The main finding of this study is that the IIR, a normalized measure of atrial myocardial LGE, is strongly associated with EAM bipolar voltage measures. To the extent that voltage amplitude correlates with atrial scar,[8, 9] determination of the IIR can be used to non-invasively assess the presence and extent of atrial scar. Compared with estimation of scar based on image intensity in typical “arbitrary units” with varying magnitude and scale, the IIR is a normalized measure with attributes that optimize a) quantification, b) reproducibility, and c) comparability between patients.

Prior Studies of Atrial LGE

Peters and colleagues initially reported the feasibility of atrial LGE imaging. In their study of 23 patients with AF, pre-ablation LGE was not observed in any patients; however, post ablation LGE was seen in all patients.[13] Subsequently, McGann and colleagues reported an 8.7% prevalence of pre-procedural LGE in a series of 46 patients.[14] The same group later reported a baseline LGE prevalence of 14.1% in patients with lone AF and 16.9% in patients with non-lone AF. In this study, the investigators categorized patients into 4 groups by the extent of pre-ablation LGE (Utah score): I with <5%, II with 5-20%, III with 20-35%, and IV with >35% atrial LGE. The authors found that the degree of atrial LGE was unassociated with AF type and comorbidities, and that extensive pre-ablation LGE was associated with a poor ablation outcome.[15] In contrast, extensive post-ablation LGE appears to be associated with procedural success.[14, 16] Follow up studies have proposed a patient specific strategy of PVI with or without linear ablations or debulking, based upon the extent of baseline LGE.[3, 17] Other studies have suggested a role for atrial LGE to assess the adequacy of ablation.[18] Taclas and colleagues, however, reported that despite a visual and quantitative association between ablation sites on EAM and LGE, 20% of ablated sites revealed no LGE.[19] Similarly, in a study of patients referred for repeat ablation, we found a significant association between LGE and low-voltage on EAM, however, LGE patterns did not identify pulmonary vein reconnection sites.[11]

Image Intensity Ratio

The above studies have made vital contributions to the understanding of the atrial arrhythmia substrate and optimal patient selection and ablation strategies. Integration of these strategies into general electrophysiology practice will likely improve patient outcomes. However, the variability of pre-ablation LGE prevalence and LGE utility for localizing ablation gaps across studies point to the suboptimal generalizability of current image analysis techniques. Prior studies have utilized dynamic (on a slice-by-slice basis) thresholds

for scar identification at 2 to 4 SD above the mean of normal tissue image intensity.[4] This methodology has been internally reproducible and has led to many important observations.[3, 17] However, the flexibility in the number of SD above normal tissue that defines scar may bias comparisons of the extent of atrial scar between patients, and limit the generalizability of this methodology at centers with less experience in LGE-MRI. The Utah score categorizes the extent of fibrosis, but the underlying continuous variable of LGE extent is similarly determined using dynamic thresholds of image intensity.[15] The IIR utilizes the mean intensity of the LA blood pool as a denominator, providing normalized results that intend to reduce the inter-patient and inter-scan variability in arbitrary unit intensities attributable to surface coil proximity (when uniformly affecting the LA), contrast dose, delay time of image acquisition after contrast injection, body mass index, hematocrit, and renal function.[6, 7] The rate-limiting image analysis step for calculation of the IIR is contouring of the LA wall, which can take up to 1 hour per patient. The remaining steps are quick to perform and generalizable to standard image analysis settings.

Validation of the IIR

Decreased electrogram voltage amplitude is an established surrogate of myocardial fibrosis.[20] We used the registration of image sectors to point-by-point sampled intra-cardiac electrograms to demonstrate that the IIR is strongly associated with electrogram voltage amplitude as a surrogate of atrial fibrosis. We also determined IIR thresholds corresponding to the commonly accepted voltage thresholds of <0.5 mV[8] and <0.1mV[9] to identify atrial fibrosis and dense scar, respectively. Importantly, the IIR threshold corresponding to typical thresholds for voltage based determination of abnormal tissue and scar were stable across patients and with increasing sample size as demonstrated in Supplemental Figure 1.

Study Limitations

Patients were heterogeneous with regard to prior ablations. However, this heterogeneity extended the range of observable scar and improved the generalizability of our data. Healthy volunteers without AF were not enrolled because intra-cardiac voltage mapping cannot be justified in the absence of planned catheter ablation. Our results may also be limited by a possibility for positional errors when registering EAM points to corresponding sectors on LGE-CMR based on the registration information obtained by the EAM software. The LGE-MRI sequence used in this study provided a 1.3 × 1.3 mm in-plane resolution and was obtained during ventricular diastole/atrial systole, thus maximizing atrial wall thickness for measurement. Nevertheless, atrial wall thickness may be near the limit of image resolution in some cases. Because of volume averaging, the analyzed LA wall sector may have included blood pool or epicardial fat in some cases. Additionally, the image sector size versus EAM voltage point field of view may not always match appropriately. The force of contact or the orientation of the mapping catheter can affect electrogram voltage on EAM and may lead to some bias. However, the strong individually clustered and pooled associations of sector IIR with voltage measures suggests that, on average, the measures represent LA myocardial tissue characteristics.

Conclusions

The IIR is closely correlated with local intra-cardiac bipolar LA voltage measures. This measure may provide utility for inter-patient and longitudinal intra-patient comparisons of LA scar burden and may ultimately improve patient selection and procedural guidance for AF ablation.

Supplementary Material

Refer to Web version on PubMed Central for supplementary material.

Acknowledgments

Funding: The study was funded by a Biosense-Webster grant and NIH grants K23HL089333 and R01HL116280 to Dr. Nazarian, the Dr. Francis P. Chiaramonte Foundation, and The Norbert and Louise Grunwald Cardiac Arrhythmia Research Fund. The content is solely the responsibility of the authors and does not necessarily represent the official views of the National Institutes of Health.

Abbreviations

IIR	Image intensity ratio
LA	Left atrial
LGE	Late gadolinium enhancement
MRI	Magnetic Resonance Imaging
AF	Atrial fibrillation
au	Arbitrary units
BMI	Body mass index
EAM	Electro-anatomical map
GRAPPA	Generalized Auto-calibrating Partially Parallel Acquisition
MPR	Multiplanar reformatted
PVI	Pulmonary vein isolation
SD	Standard deviation
GEE	Generalized Estimating Equations

References

1. Calkins H, Brugada J, Packer DL, et al. Hrs/ehra/ecas expert consensus statement on catheter and surgical ablation of atrial fibrillation: Recommendations for personnel, policy, procedures and follow-up. A report of the heart rhythm society (hrs) task force on catheter and surgical ablation of atrial fibrillation. Heart Rhythm. 2007; 4:816–861. [PubMed: 17556213]
2. Daccarett M, McGann CJ, Akoum NW, MacLeod RS, Marrouche NF. Mri of the left atrium: Predicting clinical outcomes in patients with atrial fibrillation. Expert Rev Cardiovasc Ther. 2011; 9:105–111. [PubMed: 21166532]
3. Akoum N, Daccarett M, McGann C, et al. Atrial fibrosis helps select the appropriate patient and strategy in catheter ablation of atrial fibrillation: A de-mri guided approach. Journal of cardiovascular electrophysiology. 2011; 22:16–22. [PubMed: 20807271]
4. Oakes RS, Badger TJ, Kholmovski EG, et al. Detection and quantification of left atrial structural remodeling with delayed-enhancement magnetic resonance imaging in patients with atrial fibrillation. Circulation. 2009; 119:1758–1767. [PubMed: 19307477]
5. Beinart R, Khurram IM, Liu S, et al. Cardiac magnetic resonance t1 mapping of left atrial myocardium. Heart Rhythm. 2013; 10:1325–1331. [PubMed: 23643513]
6. Judd RM, Kim RJ. Imaging time after gd-dtpa injection is critical in using delayed enhancement to determine infarct size accurately with magnetic resonance imaging. Circulation. 2002; 106:E6–E6. [PubMed: 12105174]

7. Knowles BR, Batchelor PG, Parish V, et al. Pharmacokinetic modeling of delayed gadolinium enhancement in the myocardium. Magnetic Resonance in Medicine. 2008; 60:1524–1530. [PubMed: 19025896]
8. Verma A, Wazni OM, Marrouche NF, et al. Pre-existent left atrial scarring in patients undergoing pulmonary vein antrum isolation - an independent predictor of procedural failure. J Am Coll Cardiol. 2005; 45:285–292. [PubMed: 15653029]
9. Pappone C, Oreto G, Rosanio S, et al. Atrial electroanatomic remodeling after circumferential radiofrequency pulmonary vein ablation - efficacy of an anatomic approach in a large cohort of patients with atrial fibrillation. Circulation. 2001; 104:2539–2544. [PubMed: 11714647]
10. Rivard L, Hocini M, Rostock T, et al. Improved outcome following restoration of sinus rhythm prior to catheter ablation of persistent atrial fibrillation: A comparative multicenter study. Heart Rhythm. 2012; 9:1025–1030. [PubMed: 22342863]
11. Spragg DD, Khurram I, Zimmerman SL, et al. Initial experience with magnetic resonance imaging of atrial scar and co-registration with electroanatomic voltage mapping during atrial fibrillation: Success and limitations. Heart Rhythm. 2012; 9:2003–2009. [PubMed: 23000671]
12. Sasaki T, Miller CF, Hansford R, et al. Myocardial structural associations with local electrograms: A study of postinfarct ventricular tachycardia pathophysiology and magnetic resonance-based noninvasive mapping. Circ Arrhythm Electrophysiol. 2012; 5:1081–1090. [PubMed: 23149263]
13. Peters DC, Wylie JV, Hauser TH, et al. Detection of pulmonary vein and left atrial scar after catheter ablation with three-dimensional navigator-gated delayed enhancement mr imaging: Initial experience. Radiology. 2007; 243:690–695. [PubMed: 17517928]
14. McGann CJ, Kholmovski EG, Oakes RS, et al. New magnetic resonance imaging-based method for defining the extent of left atrial wall injury after the ablation of atrial fibrillation. J Am Coll Cardiol. 2008; 52:1263–1271. [PubMed: 18926331]
15. Mahnkopf C, Badger TJ, Burgon NS, et al. Evaluation of the left atrial substrate in patients with lone atrial fibrillation using delayed-enhanced mri: Implications for disease progression and response to catheter ablation. Heart Rhythm. 2010; 7:1475–1481. [PubMed: 20601148]
16. Badger TJ, Daccarett M, Akoum NW, et al. Evaluation of left atrial lesions after initial and repeat atrial fibrillation ablation lessons learned from delayed-enhancement mri in repeat ablation procedures. Circ-Arrhythmia Elec. 2010; 3:249–259.
17. Segerson NM, Daccarett M, Badger TJ, et al. Magnetic resonance imaging-confirmed ablative debulking of the left atrial posterior wall and septum for treatment of persistent atrial fibrillation: Rationale and initial experience. Journal of cardiovascular electrophysiology. 2010; 21:126–132. [PubMed: 19804549]
18. Reddy VY, Schmidt EJ, Holmvang G, Fung M. Arrhythmia recurrence after atrial fibrillation ablation: Can magnetic resonance imaging identify gaps in atrial ablation lines? Journal of cardiovascular electrophysiology. 2008; 19:434–437. [PubMed: 18179530]
19. Taclas JE, Nezafat R, Wylie JV, et al. Relationship between intended sites of rf ablation and post-procedural scar in af patients, using late gadolinium enhancement cardiovascular magnetic resonance. Heart Rhythm. 2010; 7:489–496. [PubMed: 20122877]
20. Sanders P, Morton JB, Kistler PM, et al. Electrophysiological and electroanatomic characterization of the atria in sinus node disease: Evidence of diffuse atrial remodeling. Circulation. 2004; 109:1514–1522. [PubMed: 15007004]

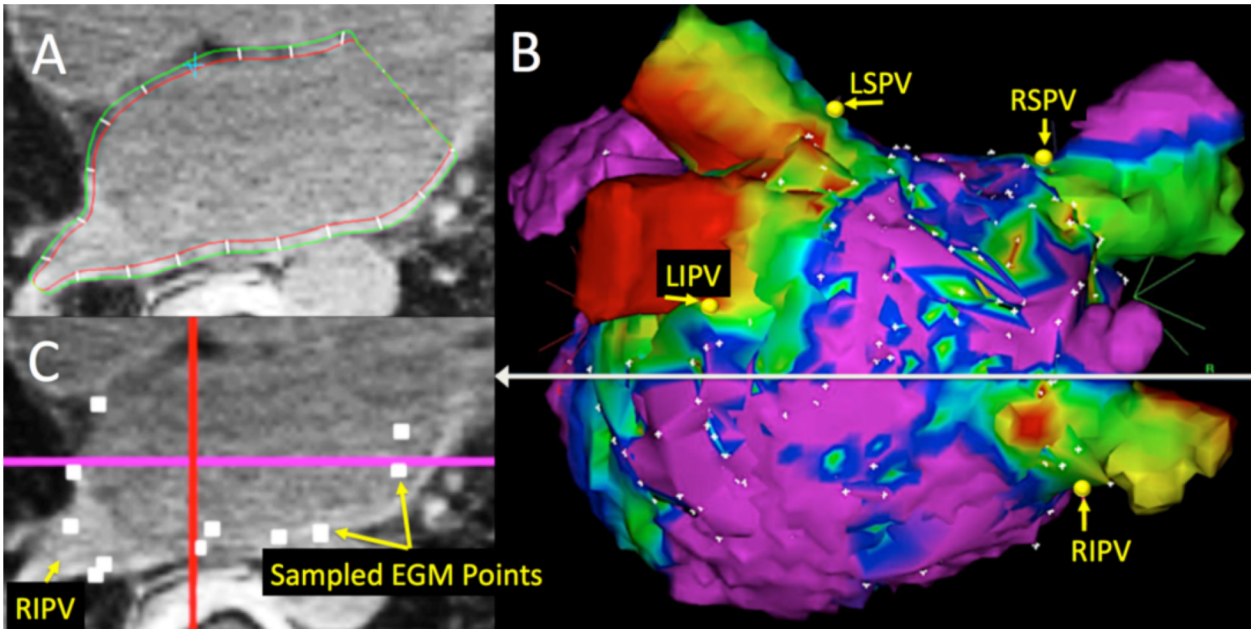

Figure 1. Example of LGE-MRI and EAM registration

Panel A: Manually drawn endo- and epicardial contours on LGE axial planes. Each plane is divided into 20 sectors within the contours, and the mean pixel intensity of each sector is calculated. Panel B: Registration of EAM points to LA angiogram using standard techniques. Antero-superior ostial left superior (LSPV) and right superior (RSPV), and antero-inferior ostial left inferior (LIPV) and right inferior (RIPV) pulmonary vein points (yellow balls) were used to merge the MR angiogram with the EAM using standard EAM system tools, thus minimizing rotational errors. Multiple posterior wall and anterior wall points (white dots) were then used for surface registration. Panel C: MPR panel corresponding to the grey line in Panel B is visualized. The merge coordinates from panel B were then utilized within the Volley software to merge the EAM with the LGE-MRI planes. Image sectors from axial planes corresponding to each EAM point (white boxes) on that plane were identified. Image intensities of each sector corresponding to EAM point voltages were recorded.

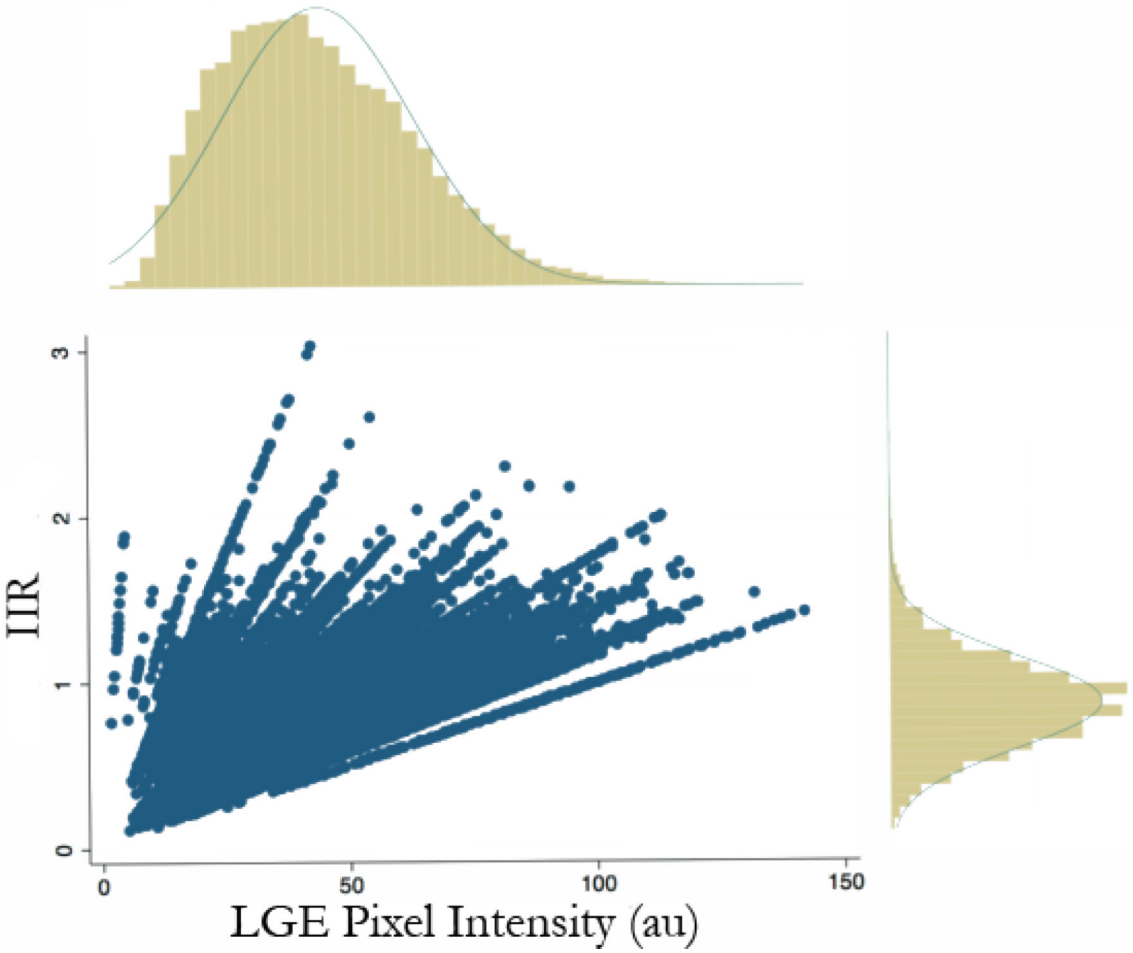

Figure 2. Distribution of image intensity versus the IIR

Plot of IIR measures on the Y-axis against corresponding image intensity (arbitrary unit - au) measures from LGE-MRI. The mean blood pool pixel intensity was 51.89±19.4 au with range from 6.7-101.1 au. The regression line slope for the association between IIR and image intensity (au) ranged from 0.01-0.16 au^{-1} among different patients. The histograms of distributions of image intensity (top) and IIR (right) are shown. In contrast to the left skewed image intensity distribution, the IIR histogram displays a normal distribution.

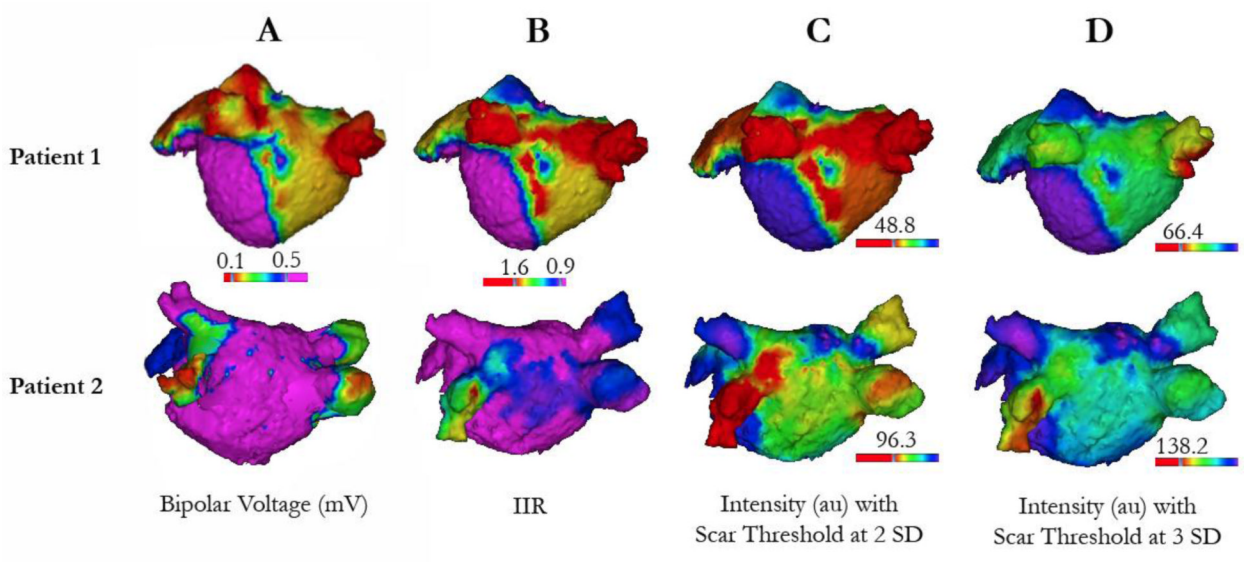

Figure 3. Qualitative examples of IIR versus voltage mapping

The figure illustrates different estimations of the extent of scar using EAM bipolar voltage (Panel A), IIR (Panel B), and intensity maps with scar threshold at 2 SD (Panel C) and 3 SD (Panel D) above the mean intensity of normal myocardium, projected onto the LA for two patients. The thresholds for scar identification (color scale) are constant across patients when using the bipolar voltage and IIR maps (Panels A and B), but vary for each patient with the dynamic intensity threshold technique (Panels C and D). Patient 1 (top row of images) exhibits large areas of low voltage on EAM indicative of fibrosis. The IIR map closely estimates the bipolar voltage map; however, the intensity maps with thresholds at 2 and 3 SD over- and under-estimate the extent of scar, respectively. Patient 2 (bottom row of images) exhibits minimal low voltage regions and predominantly healthy tissue on EAM. The IIR map closely estimates the bipolar voltage map; however, there is suboptimal agreement using dynamic intensity threshold maps at 2 and 3 SD.

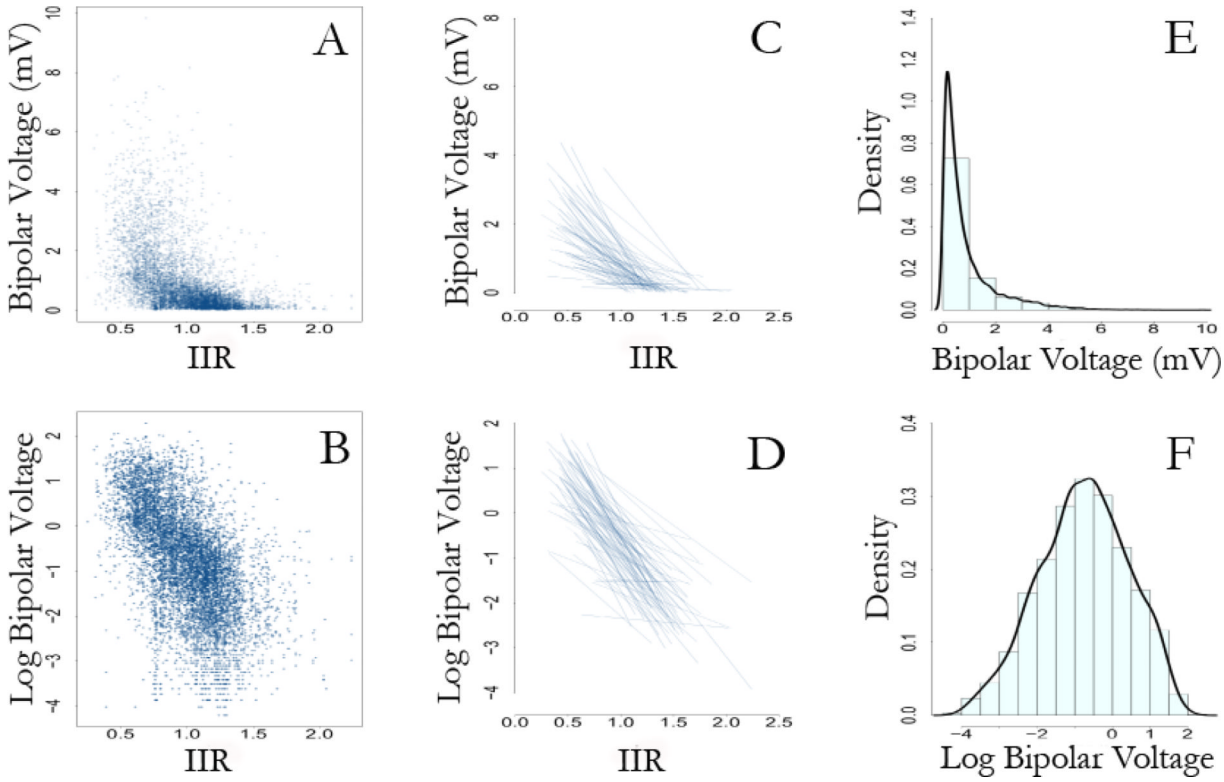

Figure 4. Distribution of voltage measures

The figure illustrates that log transformation of bipolar voltage measures accommodates modeling within a linear framework. Panel A shows a scatter plot of bipolar voltage measures against corresponding IIR values. In contrast, panel B shows the scatter plot of log transformed bipolar voltage measures versus corresponding IIR values. Panels C and D compare spaghetti plots (individual regression lines for patients) of bipolar voltage and log transformed bipolar voltage, respectively, versus the IIR values. Panel E shows the skewed distribution of bipolar voltage measures. In contrast, panel F shows the normal distribution of the log transformed bipolar voltage measures.

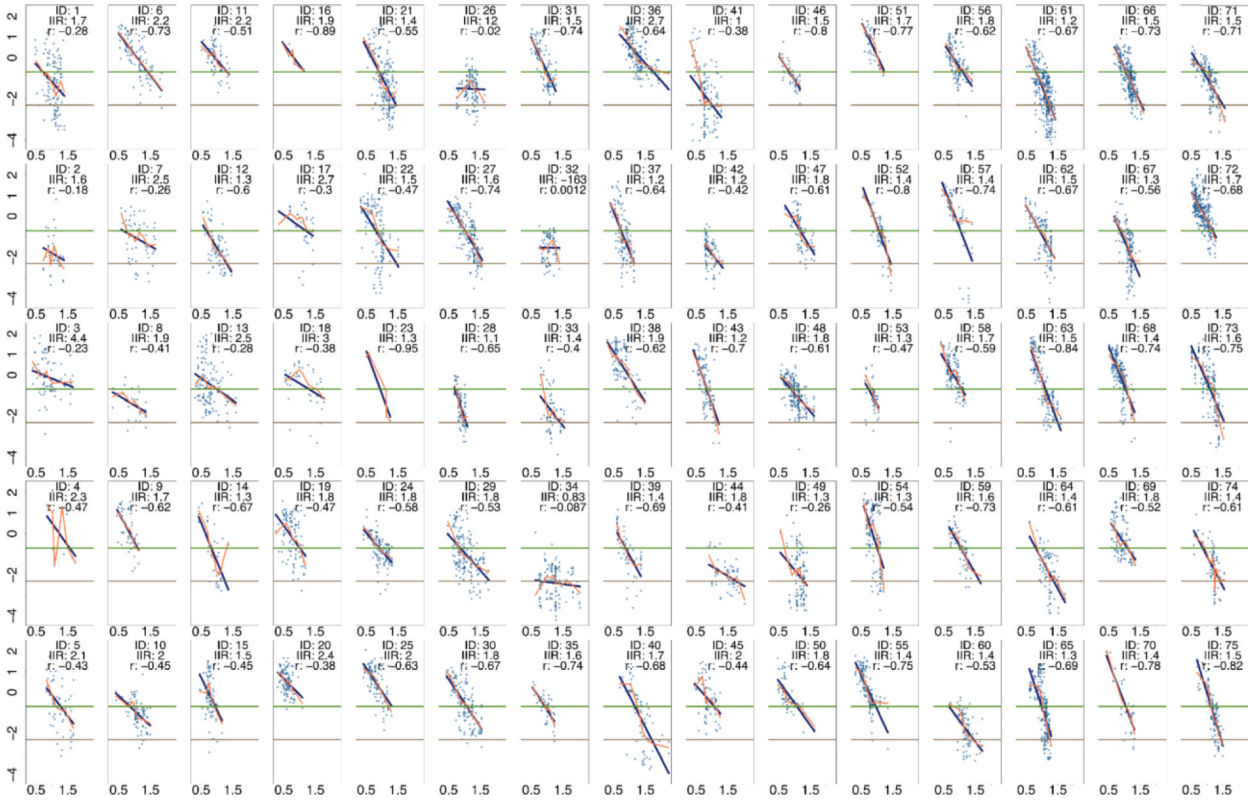

Figure 5. Clustered comparisons of IIR versus voltage

The figure illustrates 75 individual IIR versus log bipolar voltage scatterplots for each study participant identified by the ID number in each panel inset. The X-axis for each plot is IIR with values of 0.5 and 1.5 marked to show the X-axis scale. The Y-axis for each plot is log bipolar voltage. The green line corresponds to bipolar voltage = 0.5 mV, and the brown line corresponds to bipolar voltage = 0.1 mV. Each panel includes a fitted linear line (blue) and nonparametric smoothed fit (orange) line to visually demonstrate the association between IIR and log bipolar voltage measurements. Individual panel insets also include the IIR value that corresponds to the bipolar voltage threshold to identify dense scar (0.1 mV), as well as the coefficient of correlation (r) derived from each participant's regression analysis.

Table 1

Baseline Characteristics of patients

	Total	Paroxysmal AF	Persistent AF	P	First ablation	Repeat ablation	P
Patients, n	75	42	33		43	32	
Age, y	62.4±8.3	62.7±7.7	62.1±9.1	0.758	62.3±8.5	62.6±8.2	0.859
Male, n(%)	56(74.7)	30(71.4)	26(78.8)	0.467	32(74.4)	24(75.0)	0.954
Caucasian, n(%)	72(96.0)	40(95.2)	32(97.0)	0.241	42(97.7)	30(93.8)	0.492
Hypertension, n(%)	36(48.0)	21(50.0)	15(45.5)	0.696	19(44.2)	17(53.1)	0.443
Diabetes, n(%)	5(6.7)	3(7.1)	1(6.1)	0.852	3(7.0)	2(6.3)	0.901
Coronary/Vascular disease, n(%)	10(13.3)	4(9.5)	6(18.2)	0.274	5(11.6)	5(15.6)	0.615
Chronic heart failure, n(%)	11(14.7)	5(11.9)	6(18.2)	0.446	5 11.6)	6(18.8)	0.389
Prior Thromboembolism, n(%)	4(5.3)	4(9.5)	0(0)	0.068	3(7.0)	1(3.1)	0.463
Obstructive Sleep Apnea, n(%)	18(24.0)	11(26.2)	7(21.2)	0.616	13(30.2)	5(15.6)	0.143
CHA_2DS_2-VASc score	1.64±1.32	1.86±1.51	1.36±0.99		1.67± 1.52	1.59±1.01	
0, n(%)	15(20.0)	8(19.1)	7(21.2)		11(25.6)	4(12.5)	
1, n(%)	23(30.7)	12(28.6)	11(33.3)		12(27.9)	11(34.4)	
2, n(%)	21(28.0)	9(21.4)	12(36.4)	0.109	8(18.6)	13(40.6)	0.796
3, n(%)	10(13.3)	8(19.1)	2(6.1)		8(18.6)	2(6.3)	
4, n(%)	3(4.0)	2(4.8)	1(3.0)		1(2.3)	2(6.3)	
5, n(%)	2(2.7)	2(4.8)	0(0)		2(4.7)	0(0)	
6, n(%)	1(1.3)	1(2.4)			1(2.3)	0(0)	
AF Duration, years	6.6±6.8	5.6±6.5	7.8±7.0	0.166	4.9±6.3	8.9±6.8	0.011
LV Ejection Fraction, %	56.8±6.4	56.7±6.0	56.8±6.4	0.912	57.3±5.9	56.1±6.9	0.419
Prior Ablations							
None, n(%)	43(57.3)	28(66.7)	15(45.5)		43(100)	0(0)	
One, n(%)	18(24.0)	10(23.8)	8(24.2)	0.108	0(0)	18(56.3)	<0.001
Two, n(%)	13(17.3)	4(9.5)	9(27.3)		0(0)	13(40.6)	
Three, n(%)	1(1.3)	0(0)	1(3.0)		0(0)	1(3.1)	

AF = atrial fibrillation, LV = left ventricle

Table 2

LA Structural Characteristics

	Total	Paroxysmal AF	Persistent AF	P	First Ablation	Repeat Ablation	P
Patients, n	75	42	33		43	32	
LA Volume, ml	169.8±44.2	155.5±37.5	187.9±46.0	0.001	172.1±50.8	166.7±34.1	0.604
LA Volume Index, ml/m^2	83.3±20.7	78.3±18.9	89.5±21.5	0.019	84.2±23.0	82.0±17.5	0.647
LA Mass, gm	22.7±9.6	20.4±8.7	25.7±10.0	0.017	21.3±7.6	24.7±11.7	0.139
LA Mass Index, gm/m^2	11.1±4.3	10.2±4.2	12.1±4.3	0.060	10.4±3.6	11.9±5.2	0.141
LA Septal Wall Thickness, mm	2.08±0.35	2.12±0.36	2.03±0.32	0.240	2.05±0.36	2.11±0.33	0.460
LA Anterior Wall Thickness, mm	2.04±0.35	2.07±0.39	2.01±0.29	0.434	2.03±0.37	2.06±0.32	0.753
LA Posterior Wall Thickness, mm	2.27±0.39	2.30±0.40	2.24±0.37	0.491	2.26±0.39	2.28±0.39	0.815
Mean IIR	0.85±0.11	0.82±0.10	0.89±0.11	0.002	0.83±0.12	0.88±0.08	0.039
IIR-Septal Wall	0.83±0.17	0.79±0.10	0.88±0.22	0.020	0.79±0.13	0.89±0.21	0.018
IIR-Anterior Wall	0.84±0.12	0.80±0.12	0.90±0.10	<0.001	0.82±0.12	0.89±0.10	0.040
IIR-Posterior Wall	0.89±0.15	0.84±0.14	0.96±0.14	<0.001	0.88±0.17	0.91±0.11	0.514
IIR-PV Antrum	1.00±0.20	0.95±0.20	1.07±0.19	0.010	0.87±0.13	1.19±0.12	<0.001

LA= left atrium, AF= atrial fibrillation.

Table 3

Generalized Estimating Equations Model Results

Parameter	Coefficient	P
IIR	−2.44	<0.0001
Age	−0.03	0.001
Male Gender	−0.27	0.030
BMI	0.003	0.710
LA mass	0.009	0.100
LA volume	−0.0004	0.720
CHA2DS2-VASc score	0.037	0.510
AF-Persistent	−0.19	0.090
Repeat-Ablation	−0.43	<0.0001
Delay Time	0.01	0.400

IIR= image intensity ratio; LA= left atrium; BMI=body mass index; AF=atrial fibrillation.